

Macroscopic Modeling of Multiple Vehicle Types and Freeways with HOV Lanes

Alex A. Kurzhanskiy and Ajith Muralidharan

University of California, Berkeley

akurzhan@eecs.berkeley.edu, ajith@berkeley.edu

July 27, 2009

Abstract

The paper presents a way of extending the Cell Transmission Model (CTM) for road networks to accommodate multiple vehicle types and to handle freeways with high occupancy vehicle (HOV) lanes. The proposed method handles arbitrary number of vehicle types allowing to distinguish traffic by class (cars, trucks, buses), vehicle properties (hybrid, HOV), route information, or a combination of these. The freeway with HOV lane is modeled as a set of link pairs connected by nodes, where each pair consists of two parallel links, HOV and mainline (ML). The model is considered in the presence of two vehicle types, high and single occupancy. Vehicles can switch between HOV and ML links at nodes. The paper describes the distribution of flows of different vehicle types at nodes. The linear programming (LP) problem for maximization of the total node output flow is formulated and its properties are explained. Two alternative algorithms that result in suboptimal flow distribution are presented. The first one, called the “greedy” algorithm, assigns the flows picking the output links one by one, filling in the available space in one output link before going to the next. The second one distributes the flows so that the total node output flows are proportional to the available space in the downstream links. The paper considers two HOV configurations: dedicated HOV lane, where only high occupancy vehicles are allowed at all times, and time dependent HOV lane, where all vehicles are allowed at times when HOV is not active.

The methods and algorithms described in the paper are implemented and tested in Aurora Road Network Modeler, an open source software toolset for macroscopic modeling of travel corridors. Simulation results from the case study of the I-80 East freeway segment with HOV lane in Northern California are presented.

1 Introduction

As reflected in the literature, there is a considerable interest in macroscopic modeling of heterogeneous (allowing vehicles of different types) traffic on roads with special lanes where only vehicles of certain type are allowed. Extension of the Lighthill-Whitham-Richards (LWR) model to incorporate multiple lanes and different vehicle types is discussed in (9; 19). A numerical scheme for the multi-class LWR model is described in (20). Generalized theory for modeling freeways in the presence of two vehicle types with a subset of lanes reserved for one of the types based on Godunov scheme applied to the LWR equation is presented in (4) and used for simulation in (5). Introducing gas-kinetic traffic model in (8), the authors also address the issue of heterogeneous multi-lane traffic. Kinetic models of multi-class traffic on multi-lane freeway are studied in (11; 12). Macroscopic simulation for evaluation of HOV¹ lane operation, based on continuum approach that treats HOV and general purpose lanes separately with crossing points being determined from the lane changing behavior and freeway geometry, is described in (15). A multi-lane multi-class traffic flow model based on mesoscopic principles is introduced in (10). Lane changing in macroscopic setting that is consistent with car following behavior on a two-lane freeway is considered in (17). In macroscopic simulation software the support of HOV lane was implemented successfully in FREQ (7).

Aurora Road Network Modeler (RNM) (1; 14) is a tool set for operational planning and active traffic management in travel corridors (freeways and surrounding arterials), which is based on Aurora object-oriented framework (13). Aurora RNM simulator employs macroscopic Cell Transmission Model (CTM) (2; 3).

This paper is dedicated to modeling of multiple vehicle types and HOV facilities in Aurora RNM. When describing HOV implementation, we consider two different vehicle types, HOV and SOV², and discuss two types of HOV lanes, dedicated, where only HOV type vehicles are allowed, and time dependent, which is open to both vehicle types when inactive. Of particular interest is the distribution of HOV and SOV flows between HOV and general purpose lanes at nodes.

The paper is organized as follows. Section 2 describes Aurora RNM computational model with multiple vehicle types. Section 3 discusses the implementation of freeway with HOV lane. Section 4 presents a linear programming problem for flow assignment at nodes and addresses the issues of the linear programming approach. Section 5 introduces two procedures for the flow assignment that are intended to replace the

¹High Occupancy Vehicle.

²Single Occupancy Vehicle.

linear program. Section 6 provides examples showing that neither of the two procedures produces a linear programming solution in general case, and that neither of them has advantage over the other in terms of the total output flow maximization. Section 7 contains the simulation results of an I-80 East freeway segment in Northern California that has time dependent HOV lane. Section 8 concludes the paper.

2 Modeling multiple vehicle types

As described in (13), the road network consists of links and nodes, where links represent stretches of roads and nodes connect the links. A node must always have at least one input and at least one output link. A link is called an ordinary link, if it has both begin and end nodes. A link with no begin node is referred to as *source link* or *source*, and a link with no end node is called *destination link* or *sink*. Each link is characterized by its length and the fundamental diagram (capacity F , free flow speed v and congestion wave speed w), which takes into account the number of lanes. Sources are the links through which the vehicles enter the system, and therefore have demand profiles assigned to them. Each node is characterized by a split ratio matrix that determines how the incoming flows are distributed among the output links. Nodes may be used not only to represent intersections, merge, or diverge points, but also to split long links into smaller sections.

The state of the system at each simulation step is described by the vehicle density in each link. For each link, the density $\vec{\rho} = (\rho^1, \dots, \rho^K)^T$ is K -dimensional vector, with K being the number of modeled vehicle types, and ρ^k representing density of vehicles of type k , $k = 1..K$. Total vehicle density for a link is computed simply as $\rho_T = \sum_{k=1}^K \rho^k$. The state update equation for a link is

$$\vec{\rho}(t+1) = \vec{\rho}(t) + \frac{\Delta t}{\Delta x} \left(\vec{f}^u(t) - \vec{f}^d(t) \right), \quad (1)$$

where Δt is the sampling period, Δx is the link length, and K -dimensional vectors $\vec{f}^u = (f^{u1}, \dots, f^{uK})^T$ and $\vec{f}^d = (f^{d1}, \dots, f^{dK})^T$ are upstream (entering the link) and downstream (exiting the link) flows respectively, where elements f^{uk} and f^{dk} correspond to flows of vehicles of type k , $k = 1..K$. For sources, $\vec{f}^u(t)$ equals demand at time step t . For sinks, $\vec{f}^d(t) = v\vec{\rho}(t) \min \left\{ 1, \frac{F}{v\rho_T(t)} \right\}$. Otherwise, $\vec{f}^u(t)$ is determined by the begin node, and $\vec{f}^d(t)$ is determined by the end node.

A node with m input and n output links has $mK \times n$ split ratio matrix $\mathcal{B} = \{\beta_{(k-1)m+i,j}\}_{k=1..K, i=1..m, j=1..n}$. This matrix is nonnegative, its elements lying in the interval $[0, 1]$, and the sum of the elements in each row equals 1. Element $\beta_{(k-1)m+i,j}$ defines the portion of the flow of vehicles of type k coming from input link i

that has to be directed into output link j . At each time step t , the input flow vectors $\vec{f}_i^d(t)$ and output flow vectors $\vec{f}_j^u(t)$, $k = 1..K$, $i = 1..m$, $j = 1..n$, for the node are computed as follows.

1. Compute supply for each output:

$$s_j(t) = \min \{F_j, w_j (\bar{\rho}_j - \rho_{Tj}(t))\}, \quad j = 1..n, \quad (2)$$

where F_j is the capacity, w_j is the congestion wave speed, $\bar{\rho}_j$ is the jam density, and $\rho_{Tj}(t)$ is the total density of the output link j .

2. Compute input demands:

$$\tilde{d}_{(k-1)m+i}(t) = v_i \rho_i^k(t) \min \left\{ 1, \frac{F_i}{v_i \rho_{Ti}(t)} \right\}, \quad k = 1..K, \quad i = 1..m, \quad (3)$$

where F_i is capacity, v_i is free flow speed, and $\rho_{Ti}(t)$ is the total density of the input link i . Quantity $\tilde{d}_{(k-1)m+i}(t)$ represents the desired flow of vehicles of type k from the input link i .

3. Compute output demands:

$$d_j(t) = \sum_{i=1}^m \sum_{k=1}^K \beta_{(k-1)m+i,j}(t) \tilde{d}_{(k-1)m+i}(t), \quad j = 1..n. \quad (4)$$

Quantity $d_j(t)$ represents the total flow that desires to enter the output link j .

4. Initialize the scaling factors $\tilde{\delta}_{(k-1)m+i}(t) = 1$ for $k = 1..K$, $i = 1..m$.

- (a) For $q = 1..n$ update scaling factor, if necessary:

$$\tilde{\delta}_{(k-1)m+i}(t) \leftarrow \begin{cases} \tilde{\delta}_{(k-1)m+i}(t), & \text{if } \forall k \in \{1..K\}, \beta_{(k-1)m+i}(t) = 0 \\ \min \left\{ \tilde{\delta}_{(k-1)m+i}(t), \frac{s_q(t)}{d_q(t)} \right\}, & \text{otherwise} \end{cases}, \quad i = 1..m, k = 1..K; \quad (5)$$

- (b) recompute input demands

$$\tilde{d}_{(k-1)m+i}(t) \leftarrow \tilde{d}_{(k-1)m+i}(t) \tilde{\delta}_{(k-1)m+i}(t) \quad (6)$$

and recompute output demands $d_j(t)$, $j = 1..n$, according to (4).

This step implements the proportional priority rule for merging links and the first-in-first-out rule for diverging links as they are stated in (3).

5. Vector of flows leaving the input link i is

$$\vec{f}_i^d(t) = \begin{pmatrix} \tilde{d}_i(t) \\ \tilde{d}_{m+i}(t) \\ \vdots \\ \tilde{d}_{(K-1)m+i}(t) \end{pmatrix}, \quad i = 1..m. \quad (7)$$

6. Vector of flows entering the output link j is

$$\vec{f}_j^u(t) = \begin{pmatrix} \sum_{i=1}^m \beta_{i,j} \tilde{d}_i(t) \\ \sum_{i=1}^m \beta_{m+i,j} \tilde{d}_{m+i}(t) \\ \vdots \\ \sum_{i=1}^m \beta_{(K-1)m+i,j} \tilde{d}_{(K-1)m+i}(t) \end{pmatrix}, \quad j = 1..n. \quad (8)$$

Aurora RNM simulation starts with given initial density vectors on all the links. At every step of the simulation, at first the input/output flow vectors are computed on all the nodes, then the state is updated on all the links using (1).

The presented vector structure for densities and flows allows arbitrary number of vehicle types to be modeled. Vehicle types can be used to represent vehicle classes, such as cars, trucks or buses; certain vehicle properties, such as occupancy (HOV or SOV), electric or hybrid; route information; or combination of these.

If type k represents vehicles of certain size, trucks for example, one should replace ρ^k with $\alpha_k \rho^k$, f^{uk} with $\alpha_k f^{uk}$, and f^{dk} with $\alpha_k f^{dk}$ in the definition of $\vec{\rho}$, \vec{f}^u and \vec{f}^d , where the weight α_k specifies how many cars are equivalent to one vehicle of type k .

If a type represents vehicles that should follow a particular route, the split ratios for this vehicle type are fixed and constant directing the corresponding flow along the given route. Aurora RNM simulation input is normally given in the form of demand profiles for source links and split ratio profiles for nodes. The ability of vehicle types to carry route information allows Aurora RNM to accept the simulation input in the form of origin-destination (OD) matrices.

3 Modeling freeway with HOV lane

To model HOV lane on freeways, we introduce two vehicle types ($K = 2$): HOV (type $k = 1$) and SOV (type $k = 2$). Since Aurora RNM allows multiple links to connect the same pair of nodes in the same direction, we replace each freeway link with two, freeway HOV and freeway mainline (ML), at locations where HOV lane is present (Figure 1). HOV and ML links are parallel, if they connect the same pair of nodes. Parallel HOV and ML links may have different per lane fundamental diagrams. Vehicles can change between HOV and ML at nodes. If it is desirable to enable switching between HOV and ML in the middle of a long parallel link pair, it is possible to create a node that would split this link pair, as does node 3 in Figure 1.

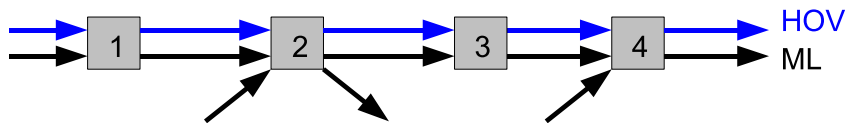


Figure 1: Freeway is represented as a set of parallel link pairs: mainline (ML) and HOV.

HOV lane is active, if only vehicles of type 1 are allowed into HOV links. There are two types of HOV facilities: a dedicated HOV lane that is active all the time, and time dependent HOV lane that is active only at certain hours during the day.

3.1 Dedicated HOV lane

Dedicated HOV lanes are present on freeways in Southern California. These HOV lanes are separated from ML by double solid line or a concrete divider. Vehicles of type 1 can cross between HOV and ML at special areas, *HOV gates*. In Aurora RNM configuration, nodes should be placed at or near HOV gate locations. If, on the other hand, a node is present where there is no HOV gate, its split ratio matrix should indicate that no crossing between HOV and ML is allowed.

For example, suppose there is no HOV gate near node 1 in Figure 1, the first input and the first output links for this node are HOV, then the split ratio matrix

$$B = \begin{pmatrix} 1 & 0 \\ 0 & 1 \\ 0 & 1 \\ 0 & 1 \end{pmatrix}$$

will ensure that no crossing between HOV and ML occurs at node 1. The fact that all SOVs are forced from HOV into ML ($\beta_{32} = 1$) is not a problem, since there should be zero SOV flow from the HOV input link.

A more interesting question is how to specify the split ratio matrix at nodes where the crossing between HOV and ML is allowed. When the split ratio matrix is well defined, that is, all its elements are nonnegative and each row sums up to 1, it determines the demand for each of the output links. This demand is determined *a priori*, meaning that no matter what the traffic state is, given portion of the flow must be directed into the specific output. In some cases (recall our example with node 1) such interpretation of the split ratio matrix is perfectly adequate. In that case, no switching between HOV and ML is allowed no matter what the traffic conditions in the downstream links.

Consider another example. Suppose, node 3 in Figure 1 is placed at the HOV gate, and vehicles of type 1 *have a choice*, which of the downstream links, HOV or ML, to take. This choice mainly depends on the traffic conditions downstream. Any *fixed* matrix \mathcal{B} eliminates the possibility of such choice. Therefore, Aurora RNM allows split ratio matrices with *undefined* elements that are computed at simulation run time based on the traffic state in the downstream links. For node 3, the split ratio matrix is partially defined:

$$\mathcal{B} = \begin{pmatrix} -1 & -1 \\ -1 & -1 \\ 0 & 1 \\ 0 & 1 \end{pmatrix}.$$

Elements in the first two rows of matrix \mathcal{B} correspond to the vehicle flows of type 1, and their negative sign indicates that they are undefined and the corresponding input-to-output flows must be assigned by the simulation. Sections 4 and 5 are devoted to flow assignment.

3.2 Time dependent HOV lane

Time dependent HOV lanes are present on freeways in Northern California. These HOV lanes are not separated from ML by any special divider, and switching between the two is allowed everywhere. Moreover, HOV lane is active only at certain time periods during the day. At other time, both vehicle types can enter HOV links.

There are two ways of modeling time dependent HOV in Aurora RNM. The obvious way, is to repeat what was done for the dedicated HOV lane with exception that now *all* nodes must act as HOV gates, and at

times when HOV lane is inactive, the structure of the split ratio matrix should permit vehicles of type 2 to switch between HOV and ML. In the example with node 3 (Figure 1), the split ratio matrix will be time dependent:

$$\mathcal{B}(t_{active}) = \begin{pmatrix} -1 & -1 \\ -1 & -1 \\ 0 & 1 \\ 0 & 1 \end{pmatrix}, \quad \mathcal{B}(t_{inactive}) = \begin{pmatrix} -1 & -1 \\ -1 & -1 \\ -1 & -1 \\ -1 & -1 \end{pmatrix}. \quad (9)$$

Here the subscripts “active” and “inactive” indicate active or inactive HOV. This approach is straight forward, since Aurora RNM admits time variant split ratio matrices.

The second way is to close HOV links at times when HOV lane is inactive while simultaneously increasing the capacity of ML:

$$F_{ML}(t_{inactive}) = F_{ML}(t_{active}) + F_{HOV}.$$

As HOV lane activates, the system returns to the usual dedicated HOV lane operation — HOV links are opened and ML capacity is reduced:

$$F_{ML}(t_{active}) = F_{ML}(t_{inactive}) - F_{HOV}.$$

Aurora RNM allows to change fundamental diagrams on links at any given time during the simulation by means of events. In the example with node 3 (Figure 1), the time dependent split ratio matrix for HOV active time will be the same as before, and for the rest of the time it will direct all the traffic to ML:

$$\mathcal{B}(t_{active}) = \begin{pmatrix} -1 & -1 \\ -1 & -1 \\ 0 & 1 \\ 0 & 1 \end{pmatrix}, \quad \mathcal{B}(t_{inactive}) = \begin{pmatrix} 0 & 1 \\ 0 & 1 \\ 0 & 1 \\ 0 & 1 \end{pmatrix}.$$

4 Flow assignment problem

4.1 Problem formulation

Now we describe the problem of flow assignment for a node with m input and n output links in a freeway system with two vehicle types, HOV and SOV, introduced in Section 3. The following notation will be used:

ρ_l^H — HOV portion of the density in link l ;

ρ_l^S — SOV portion of the density in link l ;

$\rho_{Tl} = \rho_l^H + \rho_l^S$ — total density in link l ;

v_l — free flow speed in link l ;

w_l — congestion wave speed in link l ;

$\bar{\rho}_l$ — jam density in link l ;

F_l — capacity of link l ;

f_{ij}^H — HOV flow going from the i -th input link to the j -th output link;

f_{ij}^S — SOV flow going from the i -th input link to the j -th output link;

$\mathcal{B}^H = \{\beta_{ij}^H\}$ — split ratio matrix for HOV flows;

$\mathcal{B}^S = \{\beta_{ij}^S\}$ — split ratio matrix for SOV flows.

If matrices \mathcal{B}^H and/or \mathcal{B}^S are not fully defined, the goal is to find f_{ij}^H and f_{ij}^S values that maximize the total flow leaving the node, namely

$$\sum_{i=1}^m \sum_{j=1}^n (f_{ij}^H + f_{ij}^S) \rightarrow \max. \quad (10)$$

This optimization problem must be solved under the following linear constraints:

1. input flows cannot exceed upstream demand,

$$\sum_{j=1}^n f_{ij}^H \leq v_i \rho_i^H \quad \text{and} \quad \sum_{j=1}^n f_{ij}^S \leq v_i \rho_i^S, \quad i = 1..m; \quad (11)$$

2. input flows cannot exceed upstream capacities,

$$\sum_{j=1}^n (f_{ij}^H + f_{ij}^S) \leq F_i, \quad i = 1..m; \quad (12)$$

3. output flows cannot exceed downstream supply,

$$\sum_{i=1}^m (f_{ij}^H + f_{ij}^S) \leq w_j (\bar{\rho}_j - \rho_{Tj}), \quad j = 1..n; \quad (13)$$

4. output flows cannot exceed downstream capacities,

$$\sum_{i=1}^m (f_{ij}^H + f_{ij}^S) \leq F_j, \quad j = 1..n; \quad (14)$$

5. flows cannot be negative,

$$f_{ij}^H \geq 0 \quad \text{and} \quad f_{ij}^S \geq 0, \quad i = 1..m, \quad j = 1..n; \quad (15)$$

6. first-in-first-out condition that prevents an input link to generate HOV flow when SOV flow is blocked or vice versa,

$$\rho_i^S \sum_{j=1}^n f_{ij}^H = \rho_i^H \sum_{j=1}^n f_{ij}^S, \quad i = 1..m. \quad (16)$$

Unless constraints (11), (13), and (14) limit all the flows to zero, this linear programming (LP) problem has infinitely many solutions. Additional constraints, that arise from known split ratios, may reduce the set of solutions and the objective. Suppose, certain elements of matrices \mathcal{B}^H and \mathcal{B}^S are defined: $\beta_{il}^H = \hat{\beta}_{il}^H$ and $\beta_{pq}^S = \hat{\beta}_{pq}^S$. Then, additional constraints are

$$f_{il}^H - \hat{\beta}_{il}^H \sum_{j=1}^n f_{ij}^H = 0, \quad (17)$$

and

$$f_{pq}^S - \hat{\beta}_{pq}^S \sum_{j=1}^n f_{pj}^S = 0. \quad (18)$$

7. no SOV type vehicles are allowed on the input HOV link:

$$f_{1j}^S = 0, \quad j = 1..3;$$

8. no SOV type vehicles are allowed on the output HOV link:

$$f_{i1}^S = 0, \quad i = 1..3;$$

9. off-ramp split ratios are known:

$$f_{i3}^H = \hat{\beta}^H (f_{i1}^H + f_{i2}^H + f_{i3}^H) \quad \text{and} \quad f_{i3}^S = \hat{\beta}^S (f_{i1}^S + f_{i2}^S + f_{i3}^S), \quad i = 1..3.$$

4.3 Drawback of LP

The problem with LP is that in case of multiple solutions, the choice of solution depends on the particular solver and/or its settings. For example, consider the following scenario for the two-by-two node (Figure 3), where SOV type vehicles are allowed only on links 2 and 4.

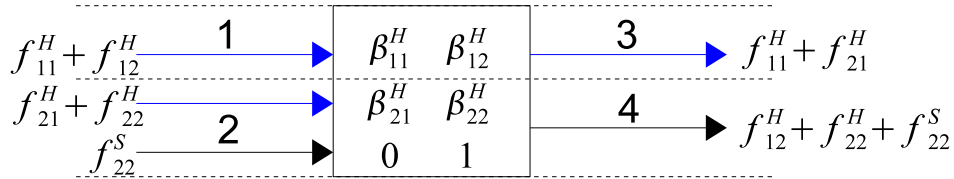


Figure 3: Node with two input and two output links: links 1 and 3 are HOV, links 2 and 4 are ML.

Figure 4 shows fundamental diagrams for the HOV links (1 and 3) and ML links(2 and 4). Links 1 (ρ_{T1}), 2 and 4 ($\rho_{T2,4}$) are in free flow. ML links have low densities. Density in link 3 (ρ_{T3}) is slightly above critical.

In this case, LP has multiple solutions. An LP solver, however, picks just one, which results in solution $\begin{pmatrix} f_{11}^H & 0 \\ f_{21}^H & 0 \end{pmatrix}$ sending vehicles to already congested HOV link.

A way to fix this obvious flaw in flow assignment, is to introduce additional constraints that would distribute the flows among the output links proportionally to the available capacity of those links. Namely, every pair of output links l and q , such that

1. there exist undefind split ratios corresponding to outputs l and q ,

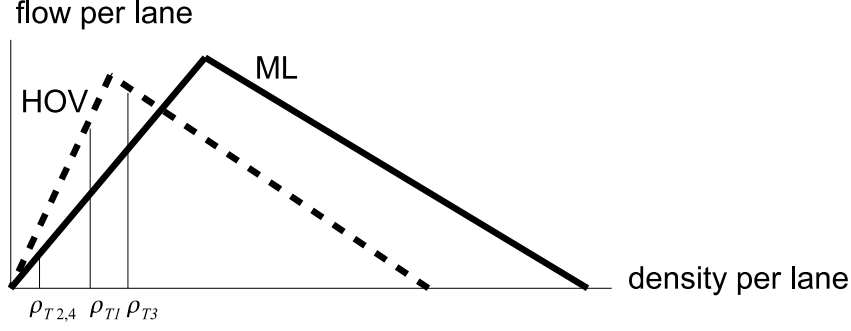


Figure 4: Fundamental diagrams for HOV and ML links: HOV link has greater free flow speed and smaller capacity.

$$2. \min \{F_l, w_l (\bar{\rho}_l - \rho_{Tl})\} > 0 \text{ and } \min \{F_q, w_q (\bar{\rho}_q - \rho_{Tq})\} > 0,$$

produces the constraint

$$\frac{\sum_{i=1}^m (f_{il}^H + f_{il}^S)}{\min \{F_l, w_l (\bar{\rho}_l - \rho_{Tl})\}} = \frac{\sum_{i=1}^m (f_{iq}^H + f_{iq}^S)}{\min \{F_q, w_q (\bar{\rho}_q - \rho_{Tq})\}}. \quad (21)$$

Constraint (21) is not absolutely harmless. Partially filled split ratio matrices may reduce the feasible set into a single point (with all flows zero), which is not physically meaningful.

Another LP issue is that in case of the input demand exceeding the output supply, the LP solution chosen by the solver may leave some input links unserved, denying any flow from those links.

The imperfection of LP prompts us to look for a *procedure* that would reasonably substitute LP by trying to maximize the total output flow of the node while producing realistic flow assignment.

5 Procedures for flow assignment

In this Section we present two algorithms for input-output flow assignment in nodes where split ratio matrices are not fully defined. The first one, the so-called “greedy” algorithm, assigns the flows picking the output links one by one, filling in the available space in one output link before switching to the next. The second one distributes the flows so that the total node output flows are proportional to the available space in the downstream links.

We consider general case: K vehicle types, and a node with m input and n output links. If a column of the split ratio matrix \mathcal{B} is fully defined, it means that flows for the corresponding output link coming from all

the input links are implicitly assigned. Therefore, without loss of generality we assume that every column of matrix \mathcal{B} has at least one undefined element⁴. It is also assumed that each row in the matrix \mathcal{B} has atleast 2 undefined elements⁵ Recall that if $\beta_{(k-1)m+i,j}(t)$ is undefined, then $\beta_{(k-1)m+i,j}(t) = -1$, $k = 1..K$, $i = 1..m$, and $j = 1..n$.

5.1 Greedy assignment

The assumption for this algorithm is that output links are ordered so that

$$\sum_{i=1}^m \sum_{k=1}^K \min \{0, \beta_{(k-1)m+i,j}(t)\} \geq \sum_{i=1}^m \sum_{k=1}^K \min \{0, \beta_{(k-1)m+i,j+1}(t)\}, \quad j = 1..n-1. \quad (22)$$

The algorithm follows.

1. Perform steps 1-2 from Section 2.
2. Compute output demands counting only entries with defined split ratios:

$$d_j(t) = \sum_{i=1}^m \sum_{k=1}^K \max \left\{ 0, \beta_{(k-1)m+i,j}(t) \tilde{d}_{(k-1)m+i}(t) \right\}, \quad j = 1..n. \quad (23)$$

It is a modified step 3 from Section 2.

3. Initialize the scaling factors $\tilde{\delta}_{(k-1)m+i}(t) = 1$ for $k = 1..K$, $i = 1..m$.

- (a) For $q = 1..n$ update scaling factor, if necessary:

$$\tilde{\delta}_{(k-1)m+i}(t) \leftarrow \begin{cases} \tilde{\delta}_{(k-1)m+i}(t), & \text{if } \forall k \in \{1..K\}, \beta_{(k-1)m+i}(t) \leq 0 \\ \min \left\{ \tilde{\delta}_{(k-1)m+i}(t), \frac{s_q(t)}{d_q(t)} \right\}, & \text{otherwise} \end{cases}, \quad i = 1..m, k = 1..K; \quad (24)$$

- (b) recompute input demands

$$\tilde{d}_{(k-1)m+i}(t) \leftarrow \tilde{d}_{(k-1)m+i}(t) \tilde{\delta}_{(k-1)m+i}(t) \quad (25)$$

and recompute output demands $d_j(t)$, $j = 1..n$, according to (4) in Section 2.

⁴If some columns of the split ratio matrix are fully defined, we first apply steps 1-4 listed in Section 2 to the corresponding output links, then, with appropriately scaled input demands, the remaining output links are treated as described in Sections 5.1 or 5.2.

⁵If only one element is undefined, it can be uniquely determined using the constraint $\sum_j \beta_{(k-1)m+i,j}(t) = 1$.

It is a modified step 4 from Section 2.

4. Set

$$\gamma_{(k-1)m+i,j}(t) = \max\{0, \beta_{(k-1)m+i,j}(t)\}, \quad k = 1..K, \quad i = 1..m, \quad j = 1..n. \quad (26)$$

5. Compute the portions of split ratios that remain unassigned for each input link and each vehicle type:

$$\bar{\beta}_{(k-1)m+i}(t) = 1 - \sum_{j=1}^n \gamma_{(k-1)m+i,j}(t), \quad k = 1..K, \quad i = 1..m. \quad (27)$$

6. Compute the remaining supply for each output link:

$$\bar{s}_j(t) = s_j(t) - d_j(t) \quad (28)$$

7. For each output link $j = 1..n$, such that $\bar{s}_j > 0$, for each input link $i = 1..m$, for each type $k = 1..K$, such that $\beta_{(k-1)m+i,j}(t) < 0$, do:

(a) define

$$\eta_{(k-1)m+i,j}(t) = \begin{cases} \bar{\beta}_{(k-1)m+i}(t), & \text{if } \tilde{d}_{(k-1)m+i}(t) = 0 \\ \min\left\{\bar{\beta}_{(k-1)m+i}(t), \frac{\bar{s}_j(t)}{\tilde{d}_{(k-1)m+i}(t)}\right\}, & \text{otherwise} \end{cases}; \quad (29)$$

(b) update split ratio:

$$\gamma_{(k-1)m+i,j}(t) \leftarrow \gamma_{(k-1)m+i,j}(t) + \eta_{(k-1)m+i,j}(t), \quad (30)$$

remaining unassigned portion of split ratio:

$$\bar{\beta}_{(k-1)m+i}(t) \leftarrow \bar{\beta}_{(k-1)m+i}(t) - \eta_{(k-1)m+i,j}(t), \quad (31)$$

and remaining supply:

$$\bar{s}_j(t) \leftarrow \bar{s}_j(t) - \eta_{(k-1)m+i,j}(t) \tilde{d}_{(k-1)m+i}(t); \quad (32)$$

This step fills in the available space in the output links one by one. The assumption (22) is important here, because unless output links with lesser choice of input flows are served first, their supply may

end up underutilized.

8. Assign split ratios:

$$\beta_{(k-1)m+i,j}(t) = \begin{cases} \gamma_{(k-1)m+i,j}(t), & \text{if } \beta_{(k-1)m+i,j}(t) \geq 0 \\ \gamma_{(k-1)m+i,j}(t) - \frac{\bar{\beta}_{(k-1)m+i}(t)}{\sum_{j=1}^n \min\{0, \beta_{(k-1)m+i,j}(t)\}}, & \text{otherwise} \end{cases}, \quad (33)$$

$k = 1..K, i = 1..m, j = 1..n.$

In (33) the remaining unassigned split ratio portion $\bar{\beta}_{(k-1)m+i}(t)$ is divided equally among the initially undefined split ratios for vehicle type k , input link i . This formula can be replaced by

$$\beta_{(k-1)m+i,j}(t) = \begin{cases} \gamma_{(k-1)m+i,j}(t), & \text{if } \beta_{(k-1)m+i,j}(t) \geq 0 \\ \gamma_{(k-1)m+i,j}(t) + \frac{\bar{\beta}_{(k-1)m+i}(t)s_j(t)}{\sum_{j=1}^n s_j(t)}, & \text{otherwise} \end{cases}, \quad (34)$$

$k = 1..K, i = 1..m, j = 1..n,$

when $\bar{\beta}_{(k-1)m+i}(t)$ is divided proportionally to the original supply of the output links among the initially undefined split ratios for vehicle type k , input link i .

9. Compute input flows \vec{f}_i^d , $i = 1..m$, and output flows \vec{f}_j^u , $j = 1..n$, following steps 1-6 from Section 2.

5.2 Proportional assignment

As was mentioned in Section 3.1, undefined split ratios for some vehicle types in some input links indicate that these vehicles can choose between two or more output links. The assumption is that presented with such a choice, a driver would select a downstream link with the least traffic density. The following algorithm intends to model this kind of behavior by assigning node input-output flows proportionally to the available space in the output links.

1. Perform steps 1-2 of the “greedy” algorithm from Section 5.1.
2. Perform steps 4-5 of the “greedy” algorithm from Section 5.1.

Note that this algorithm almost repeats the first steps of the “greedy” algorithm with the exception of step 3, which scales down input demands to satisfy output supply for known split ratios.

3. Set $r_{\max} = 1$, and $r_{\min} = 0$.

4. For each input link $i = 1..m$, for each vehicle type $k = 1..K$, repeat while $\bar{\beta}_{(k-1)m+i}(t) > 0$ and $r_{\max} > r_{\min}$:

(a) set

$$r_{\max} = \max_{j:\beta_{(k-1)m+i,j} < 0} \left\{ \frac{d_j(t)}{s_j(t)} \right\}, \quad \text{and} \quad r_{\min} = \min_{j:\beta_{(k-1)m+i,j} < 0} \left\{ \frac{d_j(t)}{s_j(t)} \right\}, \quad (35)$$

and denote

$$\hat{j} = \arg \min_{j:\beta_{(k-1)m+i,j} < 0} \left\{ \frac{d_j(t)}{s_j(t)} \right\}; \quad (36)$$

(b) define

$$\eta_{(k-1)m+i,\hat{j}}(t) = \begin{cases} \bar{\beta}_{(k-1)m+i}(t), & \text{if } \tilde{d}_{(k-1)m+i}(t) = 0 \\ \min \left\{ \bar{\beta}_{(k-1)m+i}(t), \frac{r_{\max}s_{\hat{j}}(t) - d_{\hat{j}}(t)}{\tilde{d}_{(k-1)m+i}(t)} \right\}, & \text{otherwise} \end{cases}; \quad (37)$$

(c) update split ratio:

$$\gamma_{(k-1)m+i,\hat{j}}(t) \leftarrow \gamma_{(k-1)m+i,\hat{j}}(t) + \eta_{(k-1)m+i,\hat{j}}(t), \quad (38)$$

remaining unassigned portion of split ratio:

$$\bar{\beta}_{(k-1)m+i}(t) \leftarrow \bar{\beta}_{(k-1)m+i}(t) - \eta_{(k-1)m+i,\hat{j}}(t), \quad (39)$$

and demand for the output link \hat{j} :

$$d_{\hat{j}}(t) \leftarrow d_{\hat{j}}(t) + \eta_{(k-1)m+i,\hat{j}} \tilde{d}_{(k-1)m+i}(t); \quad (40)$$

The repeat loop breaks when either the split ratios are assigned ($\bar{\beta}_{(k-1)m+i}(t) = 0$), or the output demands are equally balanced with the supply of the output links ($r_{\max} = r_{\min}$). The loop sequence is assumed to ensure that the rows with least number of undefined elements are filled up first.

5. Assign split ratios using formula (34).

Comparing this step with step 8 of the “greedy” algorithm in Section 5.1, which employs (34) instead of (33), we see that in case when $\bar{\beta}_{(k-1)m+i}(t) > 0$ for some vehicle type k and some input link i , both algorithms produce the same input and the same output flows, despite possible differences in the

resulting split ratio matrices.

6. Compute input flows \vec{f}_i^d , $i = 1..m$, and output flows \vec{f}_j^u , $j = 1..n$, following steps 1-6 from Section 2.

6 Discussion

In the general case, neither of the two procedures described in the previous Section produces a solution of LP (10)-(18), because they both employ steps 1-6 from Section 2, where step 4 implements *proportional priority rule*. The constraint imposed by the proportional priority rule for merging links (see (3)) is missing from the original LP. The following simple example explains the situation.

Example 1. Consider a node with two input and two output links as shown in Figure 5. There is only one vehicle type. Demands from the input links 1 and 2 are $\tilde{d}_1 = 1800$ vehicles per hour (vph) and $\tilde{d}_2 = 2000$ vph respectively. Supply of the output link 3 is $s_3 = 1000$ vph, and supply of the output link 4 is unlimited. The split ratio matrix $\mathcal{B} = \begin{pmatrix} 1 & 0 \\ 0.1 & 0.9 \end{pmatrix}$.

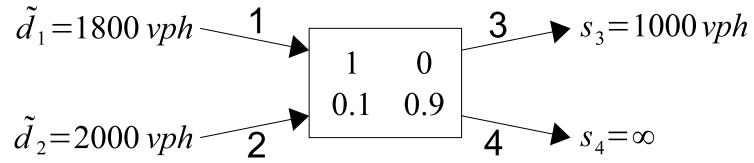


Figure 5: Node with two input and two output links, and well defined split ratio matrix.

In this example the LP has unique solution

$$f_{13} = 800, \quad f_{14} = 0,$$

$$f_{23} = 200, \quad f_{24} = 1800,$$

which results in the maximum total output flow $\sum_{i=1}^2 \sum_{j=3}^4 f_{ij} = 2800$ vph. On the other hand, following the procedure (Section 2), we first compute the output demands $d_3 = \tilde{d}_1 + 0.1\tilde{d}_2 = 2000$ vph, $d_4 = 0.9\tilde{d}_2 = 1800$ vph, and then, scale down both input demands with the *single scaling factor* $\min \left\{ 1, \frac{s_3}{d_3} \right\} = \frac{1}{2}$ according to

(5), and get the solution

$$\begin{aligned} f_{13} &= 900, & f_{14} &= 0, \\ f_{23} &= 100, & f_{24} &= 900, \end{aligned}$$

which results in the total output flow $\sum_{i=1}^2 \sum_{j=3}^4 f_{ij} = 1900$ vph. The same scaling factor $\frac{1}{2}$ for both input demands enforces the proportional priority rule: resulting input flows are proportional to the original demands ($\frac{\sum_{j=3}^4 f_{1j}}{\tilde{d}_1} = \frac{\sum_{j=3}^4 f_{2j}}{\tilde{d}_2}$).

Additional constraint

$$\frac{f_{13} + f_{14}}{\tilde{d}_1} = \frac{f_{23} + f_{24}}{\tilde{d}_2} \quad (41)$$

enforces the uniqueness of the LP solution in case of the well defined split ratio matrix, but it does not make the LP equivalent to the procedure, as it is too restrictive. For every output link where the output demand exceeds the supply all inputs are scaled down, including the ones that do not contribute to that particular output. To explain, we present the following example.

Example 2. Consider the same setup as in example 1, but with limited supply in the output link 4: $s_4 < 900$. The original LP with additional constraint (41) yields

$$\begin{aligned} f_{13} &= 1800 \frac{s_4}{1800}, & f_{14} &= 0, \\ f_{23} &= 200 \frac{s_4}{1800}, & f_{24} &= s_4, \end{aligned}$$

resulting in the total output flow $\sum_{i=1}^2 \sum_{j=3}^4 f_{ij} = \frac{19}{9}s_4$ vph. The procedure, on the other hand, requires first to scale down the input demands according to the supply of the output link 3: $\tilde{d}_1^{[1]} = 900$ and $\tilde{d}_2^{[1]} = 1000$; and then to further scale down the demand in the input link 2 according to the supply of the output link 4: $\tilde{d}_2^{[2]} = 1000 \frac{s_4}{900}$. Here, $\tilde{d}_1^{[2]} = \tilde{d}_1^{[1]}$ since this input does not contribute to the output 4 (corresponding split

ratio is 0). Hence, the solution is

$$\begin{aligned} f_{13} &= 900, & f_{14} &= 0, \\ f_{23} &= 100 \frac{s_4}{900}, & f_{24} &= s_4, \end{aligned}$$

resulting in the total output flow $\sum_{i=1}^2 \sum_{j=3}^4 f_{ij} = 900 + \frac{10}{9} s_4$ vph. Obviously, $900 + \frac{10}{9} s_4 > \frac{19}{9} s_4$.

The next question is which of the two split ratio assignment policies, “greedy” or proportional, results in the greater total output flow.

Proposition 6.1 *If the split ratio matrix is completely undefined, and “greedy” assignment produces only positive split ratios, the resulting total output flow is less or equal than the total output flow from proportional assignment.*

Proof. Denote output demands produced by “greedy” assignment d_j^g , and output demands produced by proportional assignment d_j^p , $j = 1..n$. Define total output demand $D = \sum_{j=1}^n d_j^g = \sum_{j=1}^n d_j^p$, and total output supply $S = \sum_{j=1}^n s_j$. If the output supply satisfies the demand ($D \leq S$), then the total output flow for the proportional policy is D . Otherwise, proportional policy assigns split ratios such that $\frac{d_i^p}{s_j} = \frac{D}{S}$, $j = 1..n$. According to (5), the input demands should be scaled down with scaling factor $\frac{S}{D}$ in case of proportional policy, and with scaling factor $\min_j \left\{ \frac{s_j}{d_j^g} \right\} \leq \frac{S}{D}$ in case of the greedy policy. QED.

When some of the split ratios are defined and/or there are some zero split ratios resulting from “greedy” assignment, this policy may outperform the proportional policy, as demonstrated by the next example.

Example 3. Consider a node with two input and three output links shown in Figure 6. As before, there is only one vehicle type. Demands on the input links 1 and 2 are $\tilde{d}_1 = 4000$ vph and $\tilde{d}_2 = 1000$ vph respectively. Supply of the output link 3 and 4 are $s_3 = 1000$ vph and $s_4 = 800$ vph respectively, and supply of the output link 5 is unlimited. The split ratio matrix $\mathcal{B} = \begin{pmatrix} -1 & -1 & \frac{3}{4} \\ -1 & -1 & 0 \end{pmatrix}$ — the split ratios are defined only for the output link 5.

The “greedy” assignment produces split ratio matrix $\mathcal{B}^g = \begin{pmatrix} \frac{1}{4} & 0 & \frac{3}{4} \\ 0.1 & 0.9 & 0 \end{pmatrix}$, if formula (33) is used in step

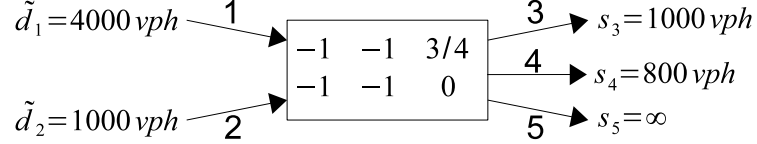


Figure 6: Node with two input and three output links, and split ratios defined only for output link 5.

8; and proportional assignment produces split ratio matrix $\mathcal{B}^p = \begin{pmatrix} \frac{5}{36} & \frac{4}{36} & \frac{3}{4} \\ \frac{5}{9} & \frac{4}{9} & 0 \end{pmatrix}$. Under “greedy” policy, at first both input demands are scaled down by the factor $\frac{s_3}{d_3} = \frac{10}{11}$ according to (5), and then the demand on the input link 2 only is scaled down by $\frac{11}{10} \frac{9}{10} \frac{800}{1000} = \frac{44}{45}$. Demand on the input link 1 is untouched because it does not contribute to the output 4. Under proportional policy, both input demands are scaled down by a single factor 0.9. So, under “greedy” policy the total output flow is $\frac{10}{11} \tilde{d}_1 + \frac{10}{11} \frac{44}{45} \tilde{d}_2 \approx 4525$ vph, whereas under proportional policy the total output flow is $0.9 (\tilde{d}_1 + \tilde{d}_2) = 4500$ vph. As we see, the “greedy” policy wins in this example because “greedy” assignment produces zero split ratio ($\beta_{14} = 0$), which is the reason for the input demands to be scaled down by two different scaling factors.

7 Application: I-80 East

Now we present some Aurora RNM simulation results of the 15-mile segment of I-80 East freeway in San Francisco Bay Area (Figure 7).



Figure 7: Map of the studied I-80 East freeway segment.

This freeway segment has a single, time dependent HOV lane, which is active from 5 to 10 AM and from 3 to 7 PM. Fundamental diagrams for the links were obtained following the calibration procedure (6; 16). HOV lane was calibrated together with ML, so the per lane fundamental diagrams of the parallel links are

the same, typically, $F/L \approx 1800$ vph per lane (L denotes the number of lanes), $v \approx 67$ mph, and $w \approx 16$ mph. Of the two ways to model freeway with HOV lane described in Section 3.2, the first one with split ratio matrices of the form (9) is used. Split ratios that direct traffic off the freeway into off-ramps are the same for both HOV and ML.

Due to the lack of exact HOV demand data, two experiments are conducted. In the first one, the HOV traffic forms 25% of the demand. Coincidentally, the lane ratio (and hence the capacity ratio) between HOV and ML is at most 1 to 3. Thus, there is no shortage of HOV vehicles during HOV active hours compared with inactive time periods, and this experiment essentially covers all the cases when the HOV traffic constitutes $\geq 25\%$ of the demand.

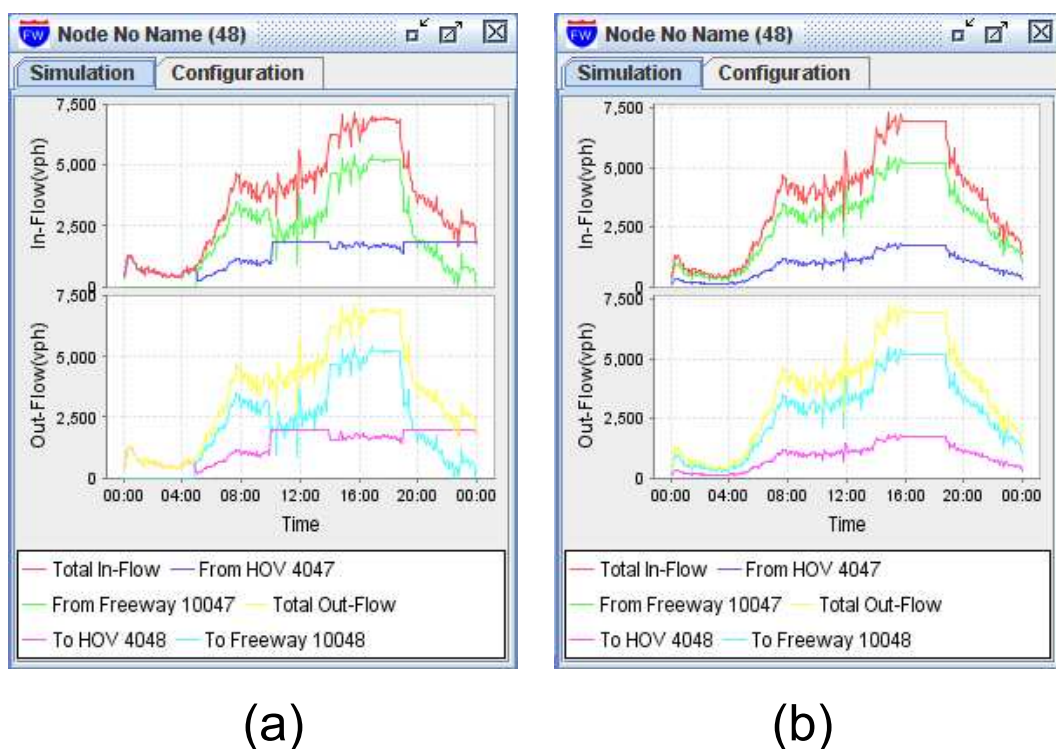
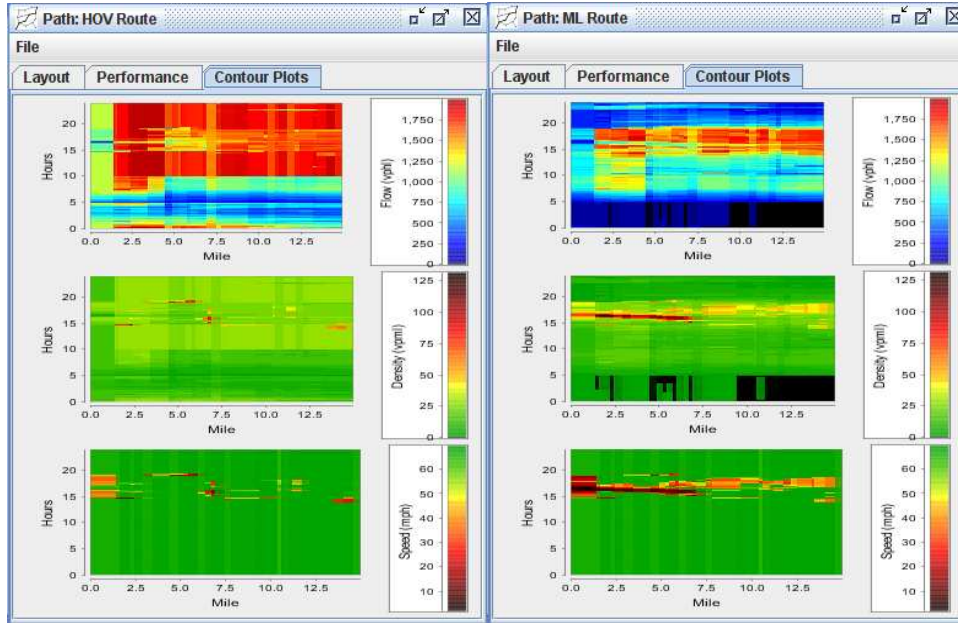


Figure 8: Node input and output flows under (a) “greedy” policy; (b) proportional policy. In the legend to the plots “From Freeway” and “To Freeway” implies “From ML” and “To ML”.

Picking any node with two input (HOV and ML) and two output (HOV and ML) links, we can compare the dynamics of the incoming and outgoing flows under “greedy” with the one under proportional flow assignment policy — see Figure 8.

Under “greedy” policy (Figure 8a), in the beginning of the day (from 0 to 5 AM), when the demand is so low that it can be satisfied by HOV lane alone, all traffic is directed into the HOV lane. Here, the order of



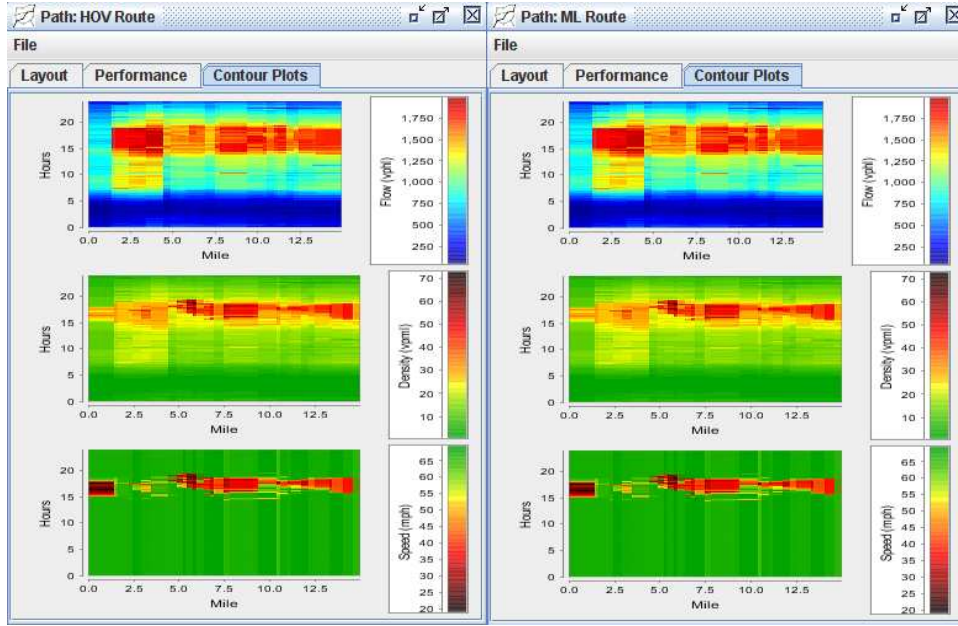
(a)

(b)

Figure 9: Flow, density and speed contours for (a) HOV and (b) ML routes under “greedy” policy.

the output links matters. In our configuration file, HOV output comes before ML output, hence, the HOV links fill up first. At 5 AM, when HOV activates, HOV flows drop while ML flows increase abruptly, and for the next five hours, until 10 AM, all HOVs stay in HOV lane, while SOVs are restricted to ML. If ML were to precede HOV in the order of output links, the picture would be entirely different: since the demand from 5 to 10 AM is low enough to be satisfied by ML only, there would be no traffic in HOV links. The HOV is inactive from 10 AM to 3 PM, so HOV flows go up while ML flows decrease at the same time. Since the demand during these hours is higher than the capacity of the HOV lane, HOV lane gets saturated — plateaus on HOV flow plots are at capacity levels of the corresponding HOV links. From 3 to 7 PM we observe the same behavior as during the morning active HOV period. The plateaus on ML flow plots correspond to periods of congestion in the ML (from 4 to 7 PM) and are below ML capacity. After 7 PM HOV flow goes up to reach the capacity level while ML flow drops to zero. If the simulation were to run longer, we would eventually see HOV flow drop as well, due to low demand at night.

Under proportional policy (Figure 8b), traffic flows behave far less dramatically. While HOV is inactive (from 0 to 5 AM, from 10 AM to 3 PM, and from 3 to 7 PM) HOV flow equals roughly $1/3$ of the ML flow, and numbers of HOVs and SOVs in both HOV and ML links are proportional to their current volumes at each time instance. During active HOV hours, almost the same proportion holds, only this time HOV lane



(a)

(b)

Figure 10: Flow, density and speed contours for (a) HOV and (b) ML routes under proportional policy.

is occupied exclusively by HOVs and ML is occupied by SOVs. The plateaus on HOV and ML flow plots correspond to periods of congestion (from 4 to 7 PM) in both HOV and ML, and each is below the respective capacity. The most important property of the proportional flow assignment is that it is *independent of the output link ordering* in a node.

Figure 9 displays flow (top), density (middle) and speed (bottom) contour plots for HOV and ML routes under “greedy” flow assignment. Here the x -axis represents route miles with traffic moving from left to right; the y -axis represents time increasing from bottom to top, and the color represents flow, density or speed value as specified by the scale to the right of each plot. Displayed flow and density values are given per lane. As flow and density contour plots indicate, during HOV inactive periods the traffic is concentrated in the HOV lane. At the afternoon peak hours HOV stays almost in free flow, while ML gets congested with speed falling down to almost zero in the upstream links. The total network delay is much greater than can be assumed by looking at speed contours, since a large queue is formed in the most upstream source link due to jammed upstream ML link.

As Figure 10 shows, under proportional flow assignment HOV contour plots are almost identical to their ML counterparts. The flows are distributed fairly, and due to the fact that in this system the HOV lane takes up 25% of the total freeway capacity almost everywhere, the HOV lane and ML with two vehicle types behave

just as a freeway where HOV is replaced with another ML lane and vehicles are not distinguished by types. Thus, the proportional policy is chosen as a default flow assignment algorithm for Aurora RNM, since it models traffic behavior realistically and does not depend on the ordering of the output links at nodes.

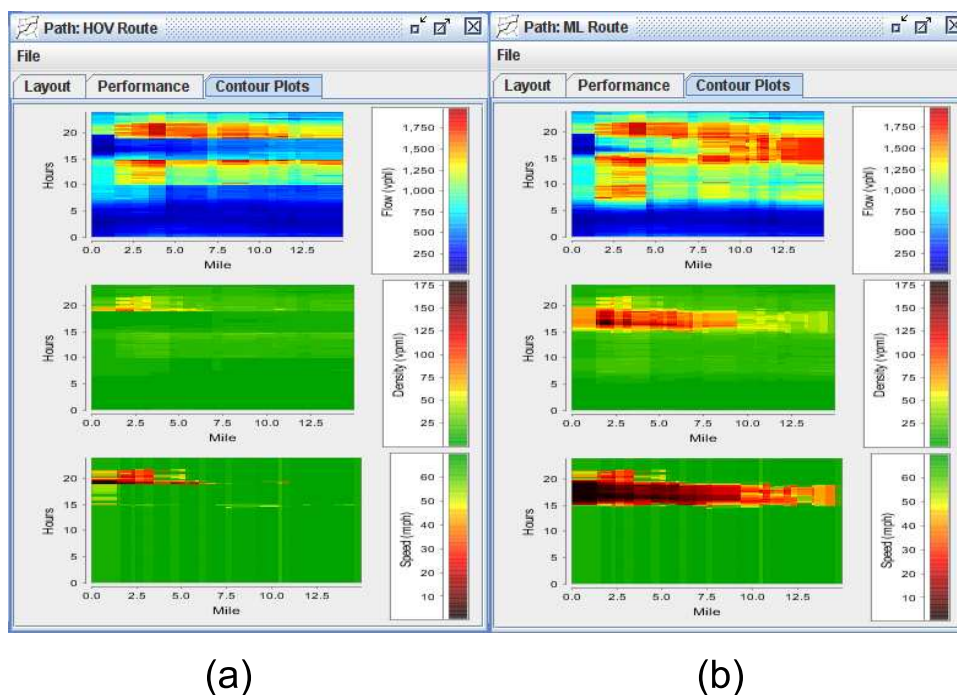


Figure 11: Flow, density and speed contours for (a) HOV and (b) ML routes under proportional policy (HOV demand is 10% of total).

In the second experiment, the HOV traffic forms only 10% of the demand. The simulation uses proportional flow assignment. Flow, density and speed contour maps for HOV and ML routes are shown in Figure 11. While HOV is inactive, the system behaves just as in the first experiment. During active HOV hours the HOV lane is underutilized due to small number of HOVs, hence the traffic volume in the HOV lane is low, and it stays in free flow. At the same time, SOV demand significantly exceeds the ML capacity, and ML gets heavily congested.

8 Conclusion

In this paper we extended the computational model employed by Aurora RNM (13; 14) to account for multiple vehicle types, where a type can represent vehicle class (car, truck or bus), describe certain vehicle properties (HOV, hybrid), or carry route information. Vehicle types that carry route information enable Aurora RNM to accept input in the form of OD matrices.

We explained how freeway with HOV lane is modeled as road network with HOV and SOV vehicle types, where nodes are connected by pairs of parallel links, HOV and ML. Vehicles can switch between HOV and ML links at nodes. During HOV active hours SOVs are restricted to ML links, while HOVs have a choice between HOV and ML links. When HOV is inactive, both HOVs and SOVs have this choice. Every node has a split ratio matrix defining the distribution of incoming flows between the output links. To indicate that vehicles of particular type coming from particular input link have a choice between two or more output links is indicated by a split ratio matrix whose elements corresponding to this vehicle type, this input and these output links, are undefined, that is, set to -1 .

The LP problem for assigning input-output flows for a node is formulated. However, even if the split ratio matrix is well defined, the formulated LP is not equivalent to steps 1-6 of the input and output flow calculation described in Section 2, because this LP does not have a constraint implementing the proportional priority rule for merging links used in step 4 of the flow calculation. As shown in Section 6, such constraint cannot be imposed in a clean way. Since the LP does not have a constraint regulating priority of merging links, it generally has infinite number of solutions, and the choice of a solution depends on particular solver and/or its settings.

Two flow assignment algorithms, “greedy” and proportional are presented as alternatives to LP. It is shown that results of both algorithms are suboptimal with respect to an LP solution. Moreover, neither of these algorithms has absolute advantage over the other in terms of maximizing the total output flow. The proportional algorithm, however, is preferable to the “greedy” one, as it is independent of the order of the output links, models traffic flows more realistically, and keeps the vehicle counts of different types in the links reasonably balanced, which is demonstrated by the I-80 East case study.

Note that both “greedy” and proportional algorithms deal with arbitrary numbers of vehicle types, input and output links. Thus, the presented HOV model can be seamlessly extended to accommodate three vehicle types — HOV, SOV and trucks. In this case, nodes will be connected by triplets of parallel links, HOV, ML and truck lane (TL), and the split ratio matrices at nodes will force trucks to stay in TL, restrict SOVs to ML and TL, and allow HOVs to be in any of the tree links.

Acknowledgement

This research is conducted within Tools for Operational Planning (TOPL) project (18) that is supported by the California Department of Transportation through the California PATH program.

References

- [1] Aurora RNM Homepage. <http://code.google.com/p/aurorarnm>.
- [2] C. F. Daganzo. The cell transmission model: A dynamic representation of highway traffic consistent with the hydrodynamic theory. *Transportation Research, B*, 28(4):269–287, 1994.
- [3] C. F. Daganzo. The cell transmission model II: Network traffic. *Transportation Research, B*, 29(2):79–93, 1995.
- [4] C. F. Daganzo. A continuum theory of traffic dynamics for freeways with special lanes. *Transportation Research, B*, 31(2):83–102, 1997.
- [5] C. F. Daganzo, W.-H. Lin, and J. M. Del Castillo. A simple physical principle for the simulation freeways with special lanes and priority vehicles. *Transportation Research, B*, 31(2):103–125, 1997.
- [6] G. Dervisoglu, G. Gomes, J. Kwon, A. Muralidharan, and P. Varaiya. Automatic calibration of the fundamental diagram and empirical observations on capacity. *88 Annual Meeting of the Transportation Research Board, Washington, D.C., USA*, 2008.
- [7] FREQ12 Homepage. <http://www.its.berkeley.edu/research/freq.html>.
- [8] D. Helbing, A. Hennecke, V. Shvetsov, and M Treiber. MASTER: macroscopic traffic simulation based on a gas-kinetic, non-local traffic model. *Transportation Research, B*, 35(2):183–211, 2001.
- [9] E. N. Holland and A. W. Woods. A continuum model for the dispersion of traffic on two-lane roads. *Transportation Research, B*, 31(6):473–485, 1997.
- [10] S. P. Hoogendoorn. *Multiclass continuum modeling of multiclass continuum flow*. PhD thesis, Delft University, 1999.
- [11] A. Klar and R. Wegener. A hierarchy of models for multilane vehicular traffic I: modeling. *SIAM Journal of Applied Mathematics*, 59(3):983–1001, 1999.
- [12] A. Klar and R. Wegener. A hierarchy of models for multilane vehicular traffic II: numerical investigations. *SIAM Journal of Applied Mathematics*, 59(3):1002–1011, 1999.
- [13] A. A. Kurzhanskiy, J. Kwon, and P. Varaiya. Aurora — Object-Oriented Framework for Simulation and Analysis of Flow Networks. 2008. Online: <http://path.berkeley.edu/topl/docs.html>.

- [14] A. A. Kurzhanskiy, J. Kwon, and P. Varaiya. Aurora Road Network Modeler. *Proceedings of the 12th IFAC Symposium on Control in Transportation Systems (to appear)*, 2009.
- [15] E. Kwon, R. Kota, and P. Michalopoulos. Macroscopic approach for evaluating diamond HOV lane operations. *79th Annual Meeting of the Transportation Research Board, Washington, D.C., USA*, 2000.
- [16] A. Muralidharan, G. Dervisoglu, and R. Horowitz. Freeway traffic flow simulation using the cell transmission model. American Control Conference, 2009.
- [17] T.-Q. Tang, S. C. Wong, H.-J. Huang, and P. Zhang. Macroscopic modeling of lane-changing for two-lane traffic flow. *Journal of Advanced Transportation*, 43(3):245–273, 2009.
- [18] TOPL Project. <http://path.berkeley.edu/topl>.
- [19] H. M. Zhang and W. L. Jin. Kinematic wave traffic flow model for mixed traffic.
- [20] M. Zhang, C.-W. Shu, G. C. K. Wong, and S. C. Wong. A weighted essentially non-oscillatory numerical scheme for a multi-class Lighthill-Whitham-Richards traffic flow model. *Journal of Computational Physics*, 191(2):639–659, 2003.